nrp **Nutrition Research and Practice**

Original Research

Check for updates

Raw *Inonotus obliquus* polysaccharide counteracts Alzheimer's disease in a transgenic mouse model by activating the ubiquitin-proteosome system

Shumin Wang [1], **Kaiye Dong** [2], **Ji Zhang** [3], **Chaochao Chen** [3], **Hongyan Shuai** [1§], **and Xin Yu** [1§]

[1]School of Basic Medicine, Dali University, Dali 671000, China
[2]Department of Ophthalmology, The First Affiliated Hospital of Dali University, Dali 671000, China
[3]College of Clinical Medicine, Dali University, Dali 671000, China

OPEN ACCESS

§**Corresponding Authors:**

Hongyan Shuai
School of Basic Medicine, Xiaguan Campus, Dali University, Wanhua Rd, Dali 671000, China.
Tel. +86-150-9696-6117
Email. shuaihy@live.com

Xin Yu
School of Basic Medicine, Xiaguan Campus, Dali University, Wanhua Rd, Dali 671000, China.
Tel. +86-172-6116-3357
Email. dalahu.cool@qq.com

ORCID iDs
Shumin Wang
https://orcid.org/0009-0002-6776-2475
Kaiye Dong
https://orcid.org/0009-0000-4621-5953
Ji Zhang
https://orcid.org/0009-0002-4485-2646

ABSTRACT

BACKGROUND/OBJECTIVES: *Inonotus obliquus* has been used as antidiabetic herb around the world, especially in the Russian and Scandinavian countries. Diabetes is widely believed to be a key factor in Alzheimer's disease (AD), which is widely considered to be type III diabetes. To investigate whether *I. obliquus* can also ameliorate AD, it would be interesting to identify new clues for AD treatment. We tested the anti-AD effects of raw *Inonotus obliquus* polysaccharide (IOP) in a mouse model of AD (3×Tg-AD transgenic mice).

MATERIALS/METHODS: SPF-grade 3×Tg-AD mice were randomly divided into three groups (Control, Metformin, and raw IOP groups, n = 5 per group). β-Amyloid deposition in the brain was analyzed using immunohistochemistry for AD characterization. Gene and protein expression of pertinent factors of the ubiquitin-proteasome system (UPS) was determined using real-time quantitative polymerase chain reaction and Western blotting.

RESULTS: Raw IOP significantly reduced the accumulation of amyloid aggregates and facilitated UPS activity, resulting in a significant reduction in AD-related symptoms in an AD mouse model. The presence of raw IOP significantly enhanced the expression of ubiquitin, E1, and Parkin (E3) at both the mRNA and protein levels in the mouse hippocampus. The mRNA level of ubiquitin carboxyl-terminal hydrolase isozyme L1, a key factor involved in UPS activation, also increased by approximately 50%.

CONCLUSIONS: Raw IOP could contribute to AD amelioration via the UPS pathway, which could be considered as a new potential strategy for AD treatment, although we could not exclude other mechanisms involved in counteracting AD processing.

Keywords: *Inonotus obliquus*; ubiquitin proteosome system; Alzheimer's disease; amyloid beta-peptides

INTRODUCTION

Alzheimer's disease (AD) is a neurodegenerative disease characterized by neuronal death and cognitive impairment, accompanied by progressive memory loss, disorientation, impaired self-care, and personality changes. It accounts for approximately 60% of all dementia cases

Chaochao Chen [ID]
https://orcid.org/0009-0002-5181-359X
Hongyan Shuai [ID]
https://orcid.org/0000-0002-9027-9046
Xin Yu [ID]
https://orcid.org/0000-0002-4860-9355

Author Contributions

Conceptualization: Wang S, Shuai H, Yu X; Data curation: Wang S, Zhang J, Chen C; Formal analysis: Wang S, Dong K, Chen C; Funding acquisition: Shuai H; Investigation: Wang S, Dong K; Methodology: Wang S, Zhang J; Project administration: Shuai H, Yu X; Resources: Dong K, Zhang J; Validation: Shuai H; Visualization: Wang S; Writing - original draft: Wang S; Writing - review & editing: Yu X.

[1]. Currently, no effective drugs are available for AD. Histopathological hallmarks of AD are intracellular neurofibrillary tangles and extracellular formation of senile plaques composed of the amyloid-beta peptide (Aβ) in aggregated form along with metal ions such as copper, iron, or zinc [2]. Although AD has a complex pathological mechanism, which is still not fully understood, the amyloid cascade hypothesis is widely accepted as a pathological explanation [3]. According to the amyloid cascade hypothesis, abnormally elevated Aβ level in the brain outside the neuronal cells may lead to the formation of fibrils rich in β-folded structures and Aβ aggregation, and then induce neurotoxicity and neurodegeneration [4]. The precursor of Aβ (amyloid precursor protein, APP) is a protein wrongly modulated after translation; however, under a powerful cellular protein quality control system, toxic or harmful coded peptides or proteins are recycled. The ubiquitin-proteasome system (UPS) is one of the major pathways of intracellular proteolysis, providing the fundamental molecular machinery for short-lived protein degradation and helping maintain overall proteostas in eukaryotic cells. Although UPS signaling is complicated and far from completely understood, one key function of the UPS is to recognize and degrade ubiquitinated and generally misfolded proteins [5]. Studies have shown that the accumulation of abnormal protein aggregates in the progressive development of AD can seriously interfere with normal protein homeostasis and the normal function of UPS, thus affecting the degradation of Aβ and leading to the formation of amyloid plaques [6-8], and the UPS was also found to ameliorate misfolded proteins in other neurodegenerative diseases.

Inonotus obliquus is a perennial macrofungus of the Polyporaceae family, with an irregular cone shape and a coke-like appearance. It is found predominantly in the cold northern regions of the Holarcticin the Northern Hemisphere [9]. It is now widely used in China, Russia, Japan, and the Nordic countries because of its active components and pharmacological effects [10]. *Inonotus obliquus* polysaccharide (IOP), the primary constituent of *I. obliquus*, has been found to have multiple functions such as anti-tumor, anti-inflammatory, anti-oxidation, anti-apoptosis, regulatory hypoglycemic/hypolipidemic effects, and neuroprotective properties [11-20]. However, it is unclear whether IOP can alleviate AD symptoms or slow down the neurodegenerative process, which has rarely been reported to date. Clarifying the beneficial effects of IOP on AD and investigating the mechanisms underlying this process would contribute to the understanding of AD progression and might contribute to the selection of new candidates for AD treatment. In this study, we investigated how raw IOP affected the physiological and biochemical indicators of triple-transgenic mouse model of AD (3×Tg-ADmouse), and our study showed that the raw IOP could effectively counteract to the symptoms in AD mice, by stimulating UPS pathway and enhanced the clearance of Aβ amyloid.

MATERIALS AND METHODS

Extraction and characterization of IOP

I. obliquus fruiting bodies collected from the Diancang Mountains (Dali, China) were extracted 3 times in 15-fold double distilled water at 70°C during a 3 h period and replaced with fresh petroleum ether for 1.5 h [21]. Extractions were combined and concentrated to an appropriate volume, deproteinized by the Sevage method (chloroform:n-butanol = 4:1, polysaccharide solution:Sevage solution = 4:1, thoroughly mixed, and deproteinized 5 times). The phenol-sulfuric acid method was used to determine the polysaccharide content of the *I. obliquus* water extract [22].

The homogeneity and molecular weight of various fractions were measured using SEC-MALLS-RI. The weight and number-average molecular weight (Mw and Mn) and polydispersity index (Mw/Mn) of various fractions in 0.1 M NaNO$_3$ aqueous solution containing 0.02% NaN$_3$ (or dimethyl sulfoxide [DMSO] solution containing 0.5% LiBr) were measured on a DAWN HELEOS-II laser photometer (Wyatt Technology Co., Santa Barbara, CA, USA) equipped with three tandem columns (300 × 8 mm, Shodex OH-pak SB-805, 804 and 803; Showa Denko K.K., Tokyo, Japan) which was held at 45°C or 60°C using a model column heater by Sanshu Biotech. Co. LTD (Shanghai, China). The flow rate was set to 0.4 mL/min (or 0.3 mL/min). A differential refractive index detector (Optilab T-rEX; Wyatt Technology Co.) was simultaneously connected to obtain the concentration of the fractions and dn/dc value. The dn/dc value of the fractions in 0.1 M NaNO$_3$ aqueous solution containing 0.02% NaN$_3$ was determined to be 0.141 mL/g, and in DMSO solution was determined to be 0.07 mL/g.

Animal and experimental design

Fifteen 12-month-old 3×Tg-AD and five C57/BL6 SPF-grade mice were obtained from the Teacher's Laboratory of Gong Zhiting, School of Basic Medical Science, Dali University (animal production license number: SYXK [Yunnan] 2018-0002). All mice were housed in cages (5 mice per cage), with constant temperature (25 ± 2°C) and light (7 AM to 7 PM) conditions. Food and water were provided to all mice throughout the study. The mice were randomly divided into 3 groups after one week of acclimatization (5 mice per group). Three groups of mice were assigned as follows: positive control group (Ctrl), metformin group (3 mg/kg/d, Met), and raw *Inonotus obliquus* polysaccharide group (6.8 g/kg/d, IOP; Ningshan Guosheng Biotechnology Co., Ltd, Shanghai, China). The mice were intragastrically administered once daily for 15 days. The C57/BL6 group was used as the control group to ensure that the mice were administered the same daily gavage volume of sterile saline. After 15 days of treatment, the mice were fasted overnight and sacrificed. Brain tissue was subsequently collected for further studies, including immunohistochemical experiments and mRNA expression analyses.

DNA extraction and identification

Total DNA was extracted from the tails of 3×Tg-AD mice using the Blood/Cell/Tissue Genome DNA Extraction Kit (Tiangen, Beijing, China) according to the manufacturer's instructions. The DNA purity was determined using an ultraviolet-visible spectrophotometer (Mio Instrument Co., Ltd, Hangzhou, China). Polymerase chain reaction (PCR) was performed using Gold Mix (green) (Tsingke Biotechnology Co., Ltd., Beijing, China) and primers were synthesized by Shanghai Sangon (Shanghai, China). PCR primers were designed using the Primer3 software. The primer sequences were used as follows: Psenl, forward: AGGCAGGAAGATCACGTGTTCAAGTAC, reverse: CACACGCACACTCTGACATGCACAGGC; APP, forward: ACCCACTGATGGTAATGCT, reverse: TCTCTCTCGGGGGTGCTTGG; tau, forward: TCGCAGTCACCGCCACCAC, reverse: TGTCATCGCTTCCAGTCCCGTC. The PCR products were analyzed by 1.5% agarose gel electrophoresis and observed under ultraviolet light.

Immunohistochemical experiments

Initially, the brains were removed, fixed in 4% paraformaldehyde solution at 4°C overnight, then dehydrated with 30% sucrose solution, and embedded in optimal cutting temperature compound. Brain sections of 30 μm thickness were sliced using a cryostat (Thermo Fisher Scientific, Waltham, MA, USA). Sections were selected from each brain and incubated overnight with a mouse anti-Aβ$_{42}$ antibody (1:200, sc28365; Santa Cruz Biotechnology,

Santa Cruz, CA, USA). They were then incubated with a biotinylated mouse secondary antibody (1:250, Immunohistochemistry SABC kit [BL733A]) for another 0.5 h, followed by staining with streptavidin-biotin complex/horseradish peroxidase (HRP). Finally, antigen-antibody complexes were detected using the avidin-biotin peroxidase method with diaminobenzidine (DAB) as a chromogenic substrate (Vectastain ABC kit, Vector Laboratories, Burlingame, CA, USA). Subsequently, the tissue samples were counterstained with hematoxylin (Beijing Zhongshan Jinqiao Biotechnology Co., Ltd., Beijing, China), dehydrated with a gradient of alcohol (75% ethanol, 95% ethanol, and absolute ethanol), sealed with neutral resin, and observed under a microscope (Olympus Optical Co., Tokyo, Japan). The integrated optical density (IOD) of the positively stained areas was quantified and analyzed using the ImageJ software.

Real-time quantitative polymerase chain reaction (RT-qPCR)

Total RNA was extracted from the mouse brain tissue using the Total Fast Pure Cell/Tissue RNA Isolation Kit and immediately reverse transcribed to cDNA using the HiScript II 1st Strand cDNA Synthesis Kit (Vazyme, Nanjing, China). In addition, we determined the mRNA transcript levels of ubiquitin, E1, Parkin, ubiquitin carboxyl-terminal hydrolase isozyme L1 (UCHL1), and $A\beta_{42}$ from each group using RT-qPCR assay. Glyceraldehyde 3-phosphate dehydrogenase (GAPDH) was used as an internal control. The primer sequences are listed in **Table 1**. The real-time PCR conditions were composed of a pre-denaturation cycle at 95°C for 30 s, followed by 40 cycles, each cycle consisting of 95°C for 25 s, and 60°C for 30 s. Dissociation curve analysis was performed for each reaction to guarantee amplification specificity. The $2^{-\Delta\Delta Ct}$ method was used to determine the relative gene expressions and the results displayed using histograms drawn with GraphPad Prism 8 software.

Western blot analysis

Mouse brain tissue was lysed using ice-cold RIPA lysis buffer (Solarbio, Beijing, China), and the homogenate was centrifuged at 4°C for 15 min. Protein concentration was evaluated using a BCA Protein Assay Kit (P0012; Shanghai Biyuntian Bioengineering Co., Ltd., Shanghai, China). Protein lysates were separated by sodium dodecyl sulfate polyacrylamide gel electrophoresis and transferred onto polyvinylidene fluoride membranes. The membranes were blocked and then incubated with primary antibody, β-actin (1:5,000) (AC004, mouse mAb, ABclonal, Woburn, MA, USA), Parkin (1:1,000) (A0968, rabbit mAb; ABclonal), UCHL1 (1:1,000) (sc-271639, mouse mAb; Santa Cruz Biotechnology), overnight at 4°C. The membranes were subsequently incubated with secondary antibodies, HRP-conjugated anti-mouse (HA1006, mouse pAb; HuaBio, Woburn, MA, USA) and anti-rabbit

Table 1. Primers sequences for real-time quantitative polymerase chain reaction

Gene	Size (bp)	Prim sequence (5′-3′)
Ubiquitin	151	F: TTAACGGACGCTTAACCGAT
		R: TTCACGTTCTCGATGGTGTC
E1	192	F: AGTACAGGGCATGATCCAAC
		R: ACAAAGTCAGGCTCTACCAG
Parkin	86	F: TTCCGAATCACCTGACGGTT
		R: ATGACTTCTCCTCCGTGGT
UCHL1	186	F: TGCTTGTTTCTGCTCCCGTCT
		R: CACTTTGTTCAGCATCTCGGGGTT
Aβ42	109	F: GATGCAGAATTCCGACATG
		R: CCACCATGAGTCCAATGAT
GAPDH	186	F: CAACTCCCACTCTTCCACCT
		R: CTTGCTCAGTGTCCTTGCTG

E1, ubiquitin-activated enzyme; UCHL1, ubiquitin carboxyl-terminal hydrolase 1; Aβ, amyloid-β protein; GAPDH, glyceraldehyde 3-phosphate dehydrogenase.

antibody (AS014, rabbit pAb; ABclonal) for 1 h at room temperature, and developed with ECL chemiluminescent detection reagent subsequently (Yisheng Biotechnology Co., Ltd, Shangha, China), β-actin was taken as loading control, the Image J software was served for quantification analysis.

Statistical analysis

The experimental data obtained from three independent experiments are presented as the mean ± standard error of the mean (SEM), and GraphPad Prism 8 software was used to calculate the P value. The Kolmogorov-Smirnov test was performed to test variables for normality, in which $P > 0.05$ indicated normally distributed data. The t-test was used for comparison between 2 groups, and the variation in multiple groups was analyzed using a one-way analysis of variance (Bonferroni method).

RESULTS

The extraction and characterization of raw IOP

The IOP extraction rate was 11.2%. The polysaccharides were subsequently precipitated using 75% alcohol, resulting in a yield of 73.8%. The average molecular weight of IOP was 2.23×10^4 Da (**Fig. 1A**) and was composed of Fuc, Rha, Ara, Gal, Glc, Xyl, Man, and Glc-UA at 12.25%, 1.90%, 0.93%, 26.35%, 43.06%, 0.87%, 7.37%, and 7.28%, respectively (**Fig. 1B**).

Aβ deposited in 3×Tg-AD mouse model

The Aβ deposition is one of the most important hallmarks of AD in the hippocampus of 3×Tg-AD mice (**Fig. 2A and B**), while the deposition of Aβ and phosphorylated tau protein triggers a series of reactions, including gliosis and synaptic dysfunction, resulting in neurodegeneration [23]. In 3×Tg-AD mice compared with C57/BL6 control mice (**Fig. 2A**), the level of $Aβ_{42}$ in the hippocampus was significantly increased in the positive control group ($P < 0.001$), which was approximately 6 times higher than that in control mice (**Fig. 2C**), as depicted in **Fig. 2A-C**. The 3×Tg-AD transgenic mice were characterized as an animal model of AD with high brain amyloid deposits and genotype-related changes.
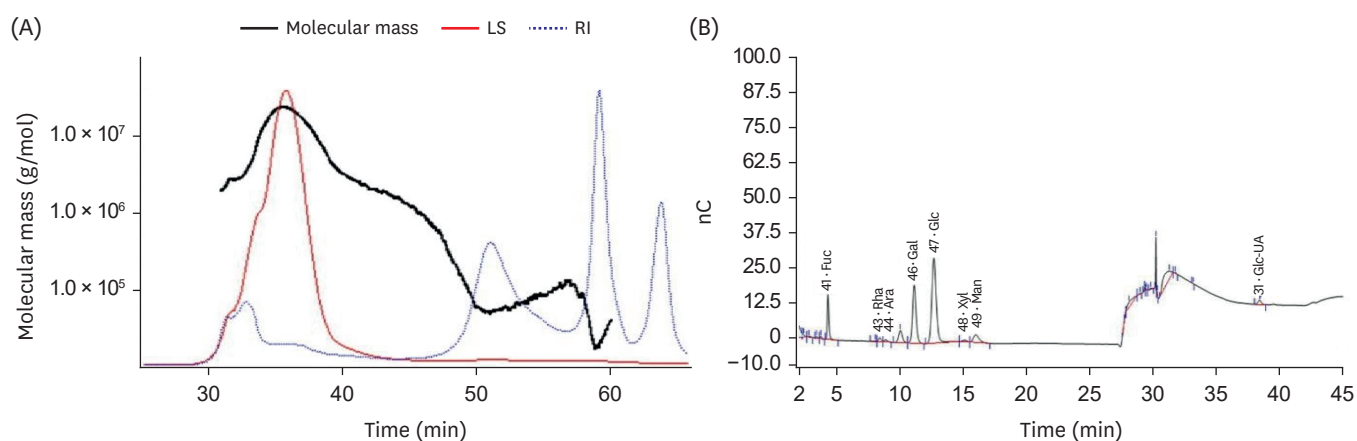

Fig. 1. The extraction and characterization of raw IOP.
(A) Molecular weight of various fractions was measured using SEC-MALLS-RI. (B) The extracts were analyzed by high-performance anion-exchange chromatography on a CarboPac PA-20 anion-exchange column to determine the composition of IOP.
IOP, *Inonotus obliquus* polysaccharide; LS, light scattering; RI, refractive index.
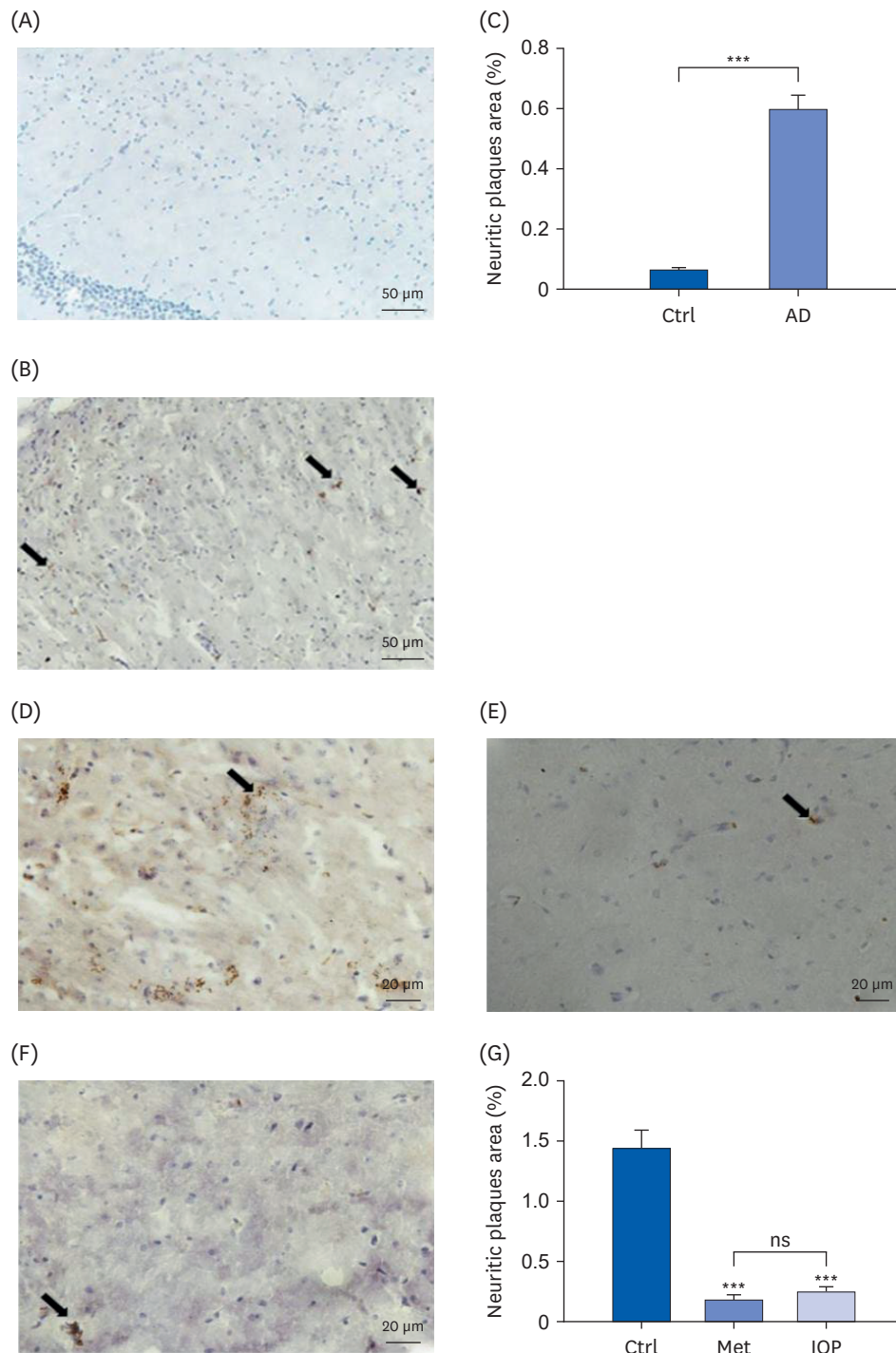
Fig. 2. Raw IOP could ameliorate the amyloid-beta deposition in AD mice.
(A) The deposition of $A\beta_{42}$ in the hippocampus of C57/BL6 mice (×20) as normal control. (B) $A\beta_{42}$ deposition (indicated by black arrow) in the hippocampus of 3×Tg-AD mice (×20). (C) Quantitative analysis of neuroinflammatory plaques in A and B. The C57/BL6 mice were taken as a normal control to 3×Tg-AD mice, [***]$P < 0.001$. (D) The deposition of $A\beta_{42}$ in the hippocampus of mice in Ctrl group. (E) The deposition of $A\beta_{42}$ in the hippocampus of mice in Met group. (F) The deposition of $A\beta_{42}$ in the hippocampus of mice in IOP group. (G) Quantitative analysis of neuroinflammatory plaques in A, B and C. [***]$P < 0.001$, compared with Ctrl group.
Three groups of mice were assigned as follows: positive control group (Ctrl), metformin group (Met), and raw *Inonotus obliquus* polysaccharide group (IOP).
IOP, *Inonotus obliquus* polysaccharide; AD, Alzheimer's disease; $A\beta$, amyloid-beta peptide; ns, not significant.

Raw IOP ameliorated the deposition of Aβ$_{42}$ on hippocampus in 3×Tg-AD mice

To verify the efficacy of raw IOP as a potential therapeutic candidate for AD, we conducted the *in vivo* study using 3×Tg-AD transgenic mice gavaged with distilled water, metformin (3 mg/kg/d), or raw IOP(6.8 g/kg/d) for 15 days. The expression of Aβ$_{42}$ levels in the brain tissues of 3×Tg-AD mice were analyzed by immunofluorescence staining. As shown in **Fig. 2D-G**, immunohistochemistry analysis of the Aβ$_{42}$ by antibody shows brown deposits in the cytoplasm under microscopy (**Fig. 2D**). Compared with the blank control group without intervention, hippocampal positive neurons were slightly lighter stained and sparser in the Met and IOP groups ($P < 0.001$) (**Fig. 2E and F**). Therefore, our results indicated that raw IOP feeding could improve Aβ$_{42}$ deposition in the brain tissue of the 3×Tg-AD mouse model. The ameliorative effects of IOP on Aβ amyloidosis were similar to those of metformin, a typical antidiabetic medicine used in the clinic (**Fig. 2G**).

UPS impairments detected in 3×Tg-AD mice

A previous study revealed that UPS impairment occurs long before the formation of β-amyloid plaques, suggesting that the formation of senile plaques may be a progressive process and that neuropathological alterations may take longer than previously thought [24]. To further examine whether the UPS was impaired in brain regions of 3×Tg-AD mice, we performed RT-qPCR analysis of the mRNA levels of UPS-related genes. As shown in **Fig. 3A-D**, compared with the blank control group, the mRNA expression levels of ubiquitin, UCHL1, E1 and Parkin (E3) were significantly downregulated in the 3×Tg-AD group ($P < 0.05$). This also indicated that the UPS was impaired or dysfunctional in the brain tissue of the 3×Tg-AD mouse model.

Raw IOP counter acted to UPS impairment by recovering the mRNA expression of UPS related genes in mouse hippocampus

The UPS degrades Aβ and has a significant effect on Aβ toxicity [7]. The expression levels of key enzymes and proteins, such as E2-25K, HRD1, Parkin, and UCHL1, may be involved in counteracting AD [25-27]. Therefore, in our study, under treatment with raw IOP, as expected, as shown in **Fig. 3E-H**, compared with the blank control group, the mRNA expression levels of ubiquitin, E1, and Parkin (E3) were significantly elevated, while the mRNA expression levels of UCHL1 were also increased by approximately 50% in the IOP group ($P < 0.05$). Met showed the same effects on UPS stimulation by upregulating mRNA expression as the positive control, suggesting that metformin is a clinical candidate for AD treatment. The elevation of the aforementioned factors showed similar trends in UPS activation following treatment with Met and IOP. The difference between the IOP and control groups was statistically significant ($P < 0.05$). Taken together, the impairment of key factors involved in UPS regulation, such as Parkin, HRD1, and UCHL1, may affect Aβ production, whereas raw IOP promotes the expression of UPS-related genes at the gene level, thereby improving UPS function.

The effect of raw IOP on the expression of key proteins regulating UPS pathway

In addition, we detected key proteins involved in the UPS pathway in the hippocampus of 3×Tg-AD mice by western blotting, as shown in **Fig. 4**. Compared with the blank control group, the expression levels of UCHL1 and Parkin (E3) in the Met group were significantly increased ($P < 0.05$), the expression levels of E3 in the IOP group were increased ($P < 0.05$), and UCHL1 showed an increasing trend. Thus, raw IOP promoted the expression of UPS-related proteins, further illustrating its stimulatory effects on UPS function.
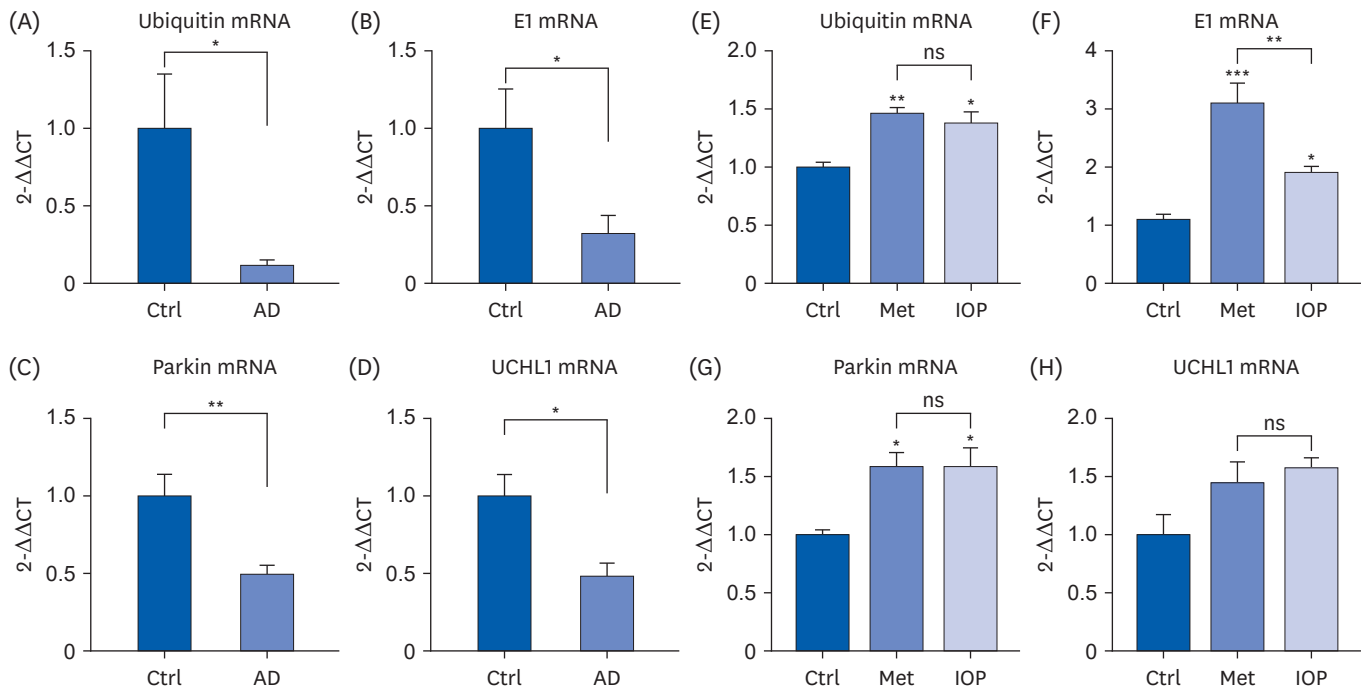
Fig. 3. Raw IOP could ameliorate the UPS impairment in AD mice.
(A) The mRNA level of ubiquitin in mice. (B) The mRNA level of E1 in mice. (C) The mRNA level of Parkin in mice. (D) The mRNA level of UCHL1 in mice (E) The mRNA level of ubiquitin in mice. (F) The mRNA level of E1 in mice. (G) The mRNA level of Parkin in mice. (H) The mRNA level of UCHL1 in mice.
Three groups of mice were assigned as follows: positive control group (Ctrl), metformin group (Met), and raw *Inonotus obliquus* polysaccharide group (IOP).
IOP, *Inonotus obliquus* polysaccharide; UPS, ubiquitin-proteasome system; AD, Alzheimer's disease; UCHL1, ubiquitin carboxyl-terminal hydrolase isozyme L1; ns, not significant.
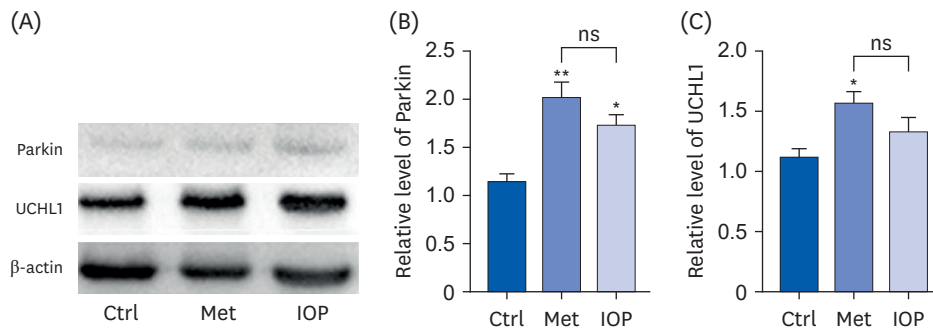*$P < 0.05$, **$P < 0.01$, ***$P < 0.001$, compared with Ctrl group.

Fig. 4. The effect of raw IOP on the expression of key proteins regulating UPS pathway.
(A) The expression of UCHL1 and Parkin in mice. (B) The quantitative analysis of Parkin in mice hippocampus. (C) The quantitative analysis of UCHL1 in mice hippocampus.
Three groups of mice were assigned as follows: positive control group (Ctrl), metformin group (Met), and raw *Inonotus obliquus* polysaccharide group (IOP).
IOP, *Inonotus obliquus* polysaccharide; UPS, ubiquitin-proteasome system; UCHL1, ubiquitin carboxyl-terminal hydrolase isozyme L1; ns, not significant.
*$P < 0.05$, **$P < 0.01$, compared with Ctrl group.

We also tested the mRNA levels of previously studied markers, including ubiquitin, E1, Parkin, and UCHL1. If significant variations in these markers could be found in AD, it would be meaningful to consider these markers for clinical diagnostic practice. Therefore, blood samples from the AD and control groups were collected for mRNA analysis. However, no significant differences were detected in the mRNA levels of ubiquitin, E1, Parkin, and UCHL1 (**Fig. 5**).
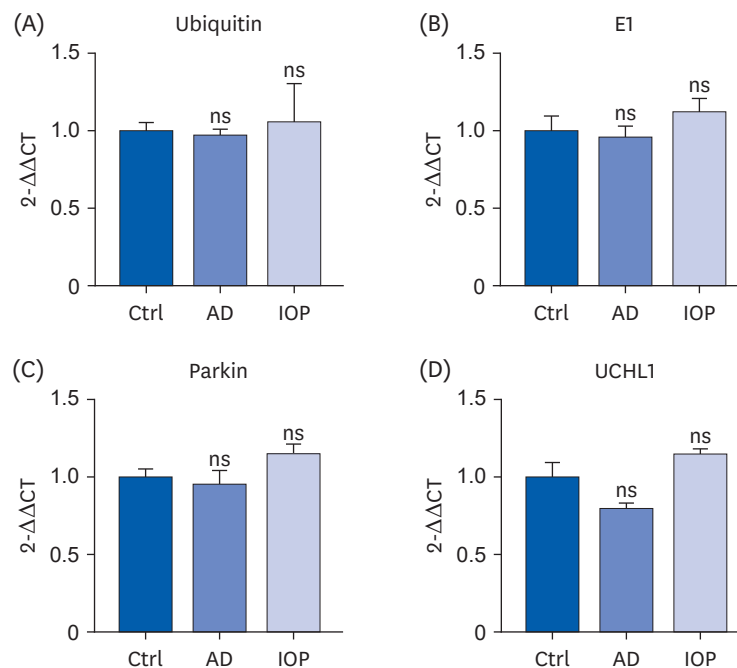
Fig. 5. The UPS regulating factors were not changed in AD mice.
Blood samples were collected and applied for UPS regulating factor analysis including ubiquitin (A), E1 (B), Parkin (C), and UCHL1 (D) by real-time quantitative polymerase chain reaction analysis under AD and IOP intervention. Three groups of mice were assigned as follows: positive control group (Ctrl), metformin group (Met), and raw *Inonotus obliquus* polysaccharide group (IOP).
UPS, ubiquitin-proteasome system; AD, Alzheimer's disease; UCHL1, ubiquitin carboxyl-terminal hydrolase isozyme L1; IOP, *Inonotus obliquus* polysaccharide; ns, not significant.

In summary, according to our study, the key factors responsible for UPS regulation, including ubiquitin, E1, Parkin, and UCHL1, were down regulated in AD at both the mRNA and protein levels. Both Met and raw IOP ameliorated UPS impairment by up regulating the expression of these factors. This study introduced a new approach to using antidiabetic herbs and functional foods to help patients with AD.

DISCUSSION

The prevention and treatment of AD remains a serious global challenge, and despite rapidly expanding efforts, no effective treatment is yet available for AD [28]. Fungal species, which contain many nutrients and bioactive compounds, are underutilized as potential candidate agents for AD treatment. In particular, IOP has gained wide acceptance in Europe and is considered by the medical community an effective source for cancer prevention and alleviating cerebrovascular diseases and diabetes [29,30]. Recent studies have suggested that endocrine abnormalities, especially diabetes, are common in AD, and AD is even regarded as type 3 diabetes [31]. Therefore, we speculated that IOP exerts positive therapeutic effects on AD, although the exact mechanism has not yet been elucidated [13]. A previous study by Han *et al.* [13] showed that IOP could significantly ameliorate oxidative stress induced in AD mice and that the application of IOP in AD mice could counteract apoptosis. Their study also supported our hypothesis that IOP could ameliorate the accumulation of Aβ amyloid. However, this study did not explain the mechanisms by which oxidative stress was induced. Our study indicated a dysfunction of the UPS and could explain how these findings were

induced in AD mice. Oxidative stress is caused by dysfunction of the ubiquitin-proteasome system, leading to harmful effects on cholinergic cells, and has been reported in other neurodegenerative diseases, including AD [32]. Therefore, we suspect that targeting the prevention of UPS dysfunction in AD is a valuable therapeutic strategy. Although IOP is traditionally used as an antidiabetic herb, we have reported its beneficial effects on the UPS in AD mouse models. Additionally, considering the beneficial effects of IOP as a functional food or herb, a thorough purification of IOP might be costly or even overqualified for functional food application; therefore, we used raw IOP in this study rather than purified IOP as reported by Han *et al.* [13], and similar beneficial effects of raw IOP were observed.

In this study, APP/PS1/tau triple-transgenic mice overexpressing mutant APP (APPSWE), PS1 (PS1M146V), or tau (tauP301L) were used to investigate the effect of raw IOP on 3×Tg-AD. The 3×Tg-AD mouse model of AD progressively develops both Aβ plaques and neurofibrillary tangles with a temporal and spatial distribution that closely mimics AD in humans [33]. Recent studies suggested that intracellular Aβ accumulation plays an important role in the pathogenesis of AD. Intracellular Aβ$_{42}$ accumulation occurs in the pyramidal neurons of the hippocampus and entorhinal cortex long before the emergence of Aβ plaques and paired helical filaments in the brains of AD patients [34]. Reducing or eliminating the production of Aβ is an important strategy for treatment, at least hindering the progression of Alzheimer's [35]. In our study, compared with the control group, the number of positively stained amyloid plaques was significantly decreased in both the Met and raw IOP groups as shown by immunohistochemical staining tests, which indicated that IOP could ameliorate the formation of toxic species of Aβ and hinder the accumulation of misfolded proteins in the brains of 3×Tg-AD mice, which was supported by the results of Garcia-Alloza *et al.* [36] and Ringman *et al.* [37]. At the meanwhile, growing evidence shows that impaired Aβ clearance appears to be one of the major causes of Aβ accumulation in late-onset sporadic AD, which accounts for over 95% of cases [38]. Therefore, it is not difficult to associate the UPS, a major intracellular proteolytic pathway that promotes the degradation of normal cellular proteins as well as the clearance of misfolded proteins [39]. The accumulations of Aβ and the hyperphosphorylation of tau, as well as neurodegeneration in AD, are closely connected with UPS dysfunction [40]. Evidence suggests that proteasome activity decreases in the brains of patients with AD [41,42]. Furthermore, a recent study showed that deficiency in UCHL1, a ubiquitin hydrolysis, induced behavioral deficits in APP-overexpressing mice [43], highlighting the importance of UPS impairments in AD mouse models. Therefore, we were interested in whether the UPS was damaged in the 3×Tg-AD mouse model, and this hypothesis was supported by the results of this study. We found that proteasome activity was impaired in the 3×Tg-AD mice. However, it remains unclear whether the accumulation of Aβ was induced by the dysfunction of UPS or the dysfunction of UPS was caused by Aβ aggregation, which is still a subject of debate relating to the pathogenesis of AD [44]. Considering the unknown correlation between Aβ and the function of UPS in AD, we hypothesized that the formation of amyloid plaques in AD mice may be a product of ubiquitin-mediated protein degradation defects. Raw IOP may play a pivotal role in Aβ clearance via the UPS pathway, thereby contributing to AD treatment.

The effective activation of the UPS has been shown to be beneficial for many diseases, especially those induced and/or tightly related to protein misfolding and aggregation, such as AD, Huntington's disease, Parkinson's disease, and various spinocerebellar ataxias [45-47]. Therefore, we suspect that the stimulation of the UPS could be a potential strategy for AD treatment. Many natural products could be beneficial for AD; however, the exact underlying mechanisms are unclear, and it would be difficult to improve the treatment

effects to fulfill clinical practice in the future. Increased IOP has been reported to counteract diabetes, which can also contribute to AD release as Met did. Therefore, in this study, Met was used as a positive control for its neuroprotective effects. We used RT-qPCR and western blotting analysis to verify that IOP exerted beneficial effects on AD via the activation of the UPS pathways. The E3 Ub protein ligases play a pivotal role in the ubiquitination reaction because they mainly determine the substrate specificity of the Ub conjugation reaction, a key regulatory process for the ubiquitination of aggregated substrates, which includes Parkin, HRD1, and UCHL-1 [48]. Lonskaya *et al.* [49] revealed that the intracellular aggregation of Aβ and damaged proteasome activity could be restored by the activation of Parkin. Furthermore, Parkin showed the capability to protect neurons, by enhancing the ubiquitination and clearance of misfolding Aβ, and it also reverses behavioral aberrations of the AD model mouse by reversing the deleterious effects of Aβ via proteosome system [50]. UCHL1 is an E3 ligase that is mainly expressed in neurons and functions as a deubiquitinating enzyme. The down regulation of both UCHL1 mRNA and UCHL1 protein has been detected in AD [26]. UCHL1 is an attractive drug target for AD; besides reducing Aβ production, UCHL1 has also been found to play an essential role in synaptic plasticity [51]. Our results showed that the expression of almost all E3 ligases, including ubiquitin, E1, and Parkin (E3), was upregulated, as was the expression of UCHL1, under Met and IOP treatment, which was supported by other studies conducted by Solano *et al* [52] and Zhang *et al.* [53]. The functions of multiple E3 ligases involved in Aβ clearance are shown in **Fig. 6**.

Although the therapeutic effect of metformin in this experiment was slightly better than that of the raw IOP extract in the mouse model, this might be due to the impurities of IOP and the unoptimized dose used in this study, which will be further studied in the future. Furthermore, the relationship between the neuroprotective properties and specific
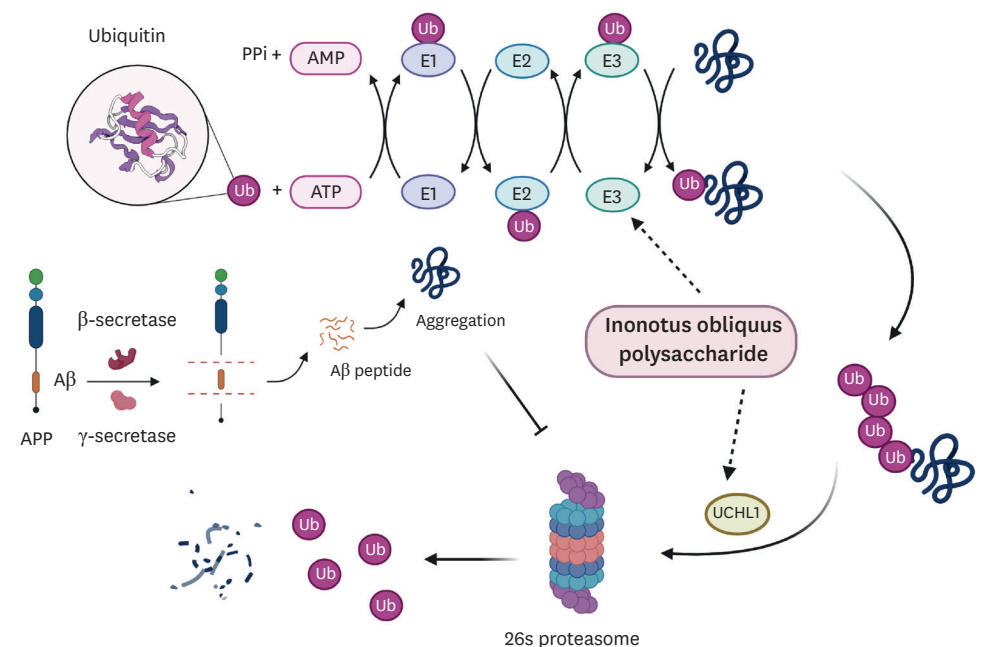

Fig. 6. Potential intervention mechanism of raw *Inonotus obliquus* polysaccharide on UPS in AD mice.
UPS, ubiquitin-proteasome system; AD, Alzheimer's disease; Ub, ubiquitin; E1, ubiquitin-activated enzyme; E2, ubiquitin-conjugating-enzyme; E3, ubiquitin–protein ligase; UCHL1, ubiquitin carboxyl-terminal hydrolase 1; APP, amyloid precursor protein; Aβ, amyloid-β protein.

ingredients of raw IOP remains unclear and requires a detailed systematic investigation. Our results provide experimental evidence supporting further investigation of IOP as a potential therapeutic candidate for AD, in addition to its beneficial function in type 2 diabetes mellitus. In conclusion, we successfully confirmed that raw IOP showed beneficial effects *in vivo* for AD treatment by promoting the intracellular degradation of Aβ via the UPS pathway.

ACKNOWLEDGMENTS

REFERENCES

1. Rusek M, Pluta R, Ułamek-Kozioł M, Czuczwar SJ. Ketogenic diet in Alzheimer's disease. Int J Mol Sci 2019;20:3892.
   PUBMED | **CROSSREF**

2. Glenner GG, Wong CW. Alzheimer's disease: initial report of the purification and characterization of a novel cerebrovascular amyloid protein. Biochem Biophys Res Commun 1984;120:885-90.
   PUBMED | **CROSSREF**

3. Selkoe DJ, Hardy J. The amyloid hypothesis of Alzheimer's disease at 25 years. EMBO Mol Med 2016;8:595-608.
   PUBMED | **CROSSREF**

4. Cheignon C, Tomas M, Bonnefont-Rousselot D, Faller P, Hureau C, Collin F. Oxidative stress and the amyloid beta peptide in Alzheimer's disease. Redox Biol 2018;14:450-64.
   PUBMED | **CROSSREF**

5. Bachiller S, Alonso-Bellido IM, Real LM, Pérez-Villegas EM, Venero JL, Deierborg T, Armengol JÁ, Ruiz R. The ubiquitin proteasome system in neuromuscular disorders: moving beyond movement. Int J Mol Sci 2020;21:6429.
   PUBMED | **CROSSREF**

6. Hong L, Huang HC, Jiang ZF. Relationship between amyloid-beta and the ubiquitin-proteasome system in Alzheimer's disease. Neurol Res 2014;36:276-82.
   PUBMED | **CROSSREF**

7. Lopez Salon M, Pasquini L, Besio Moreno M, Pasquini JM, Soto E. Relationship between beta-amyloid degradation and the 26S proteasome in neural cells. Exp Neurol 2003;180:131-43.
   PUBMED | **CROSSREF**

8. Verheijen BM, Stevens JA, Gentier RJ, van 't Hekke CD, van den Hove DL, Hermes DJ, Steinbusch HW, Ruijter JM, Grimm MO, Haupenthal VJ, et al. Paradoxical effects of mutant ubiquitin on Aβ plaque formation in an Alzheimer mouse model. Neurobiol Aging 2018;72:62-71.
   PUBMED | **CROSSREF**

9. Lee MW, Hur H, Chang KC, Lee TS, Ka KH, Jankovsky L. Introduction to distribution and ecology of sterile conks of *Inonotus obliquus*. Mycobiology 2008;36:199-202.
   PUBMED | **CROSSREF**

10. Lu Y, Jia Y, Xue Z, Li N, Liu J, Chen H. Recent developments in *Inonotus obliquus* (Chaga mushroom) polysaccharides: isolation, structural characteristics, biological activities and application. Polymers (Basel) 2021;13:1441.
    PUBMED | **CROSSREF**

11. Arata S, Watanabe J, Maeda M, Yamamoto M, Matsuhashi H, Mochizuki M, Kagami N, Honda K, Inagaki M. Continuous intake of the Chaga mushroom (*Inonotus obliquus*) aqueous extract suppresses cancer progression and maintains body temperature in mice. Heliyon (Lond) 2016;2:e00111.
    PUBMED | **CROSSREF**

12. Giridharan VV, Thandavarayan RA, Konishi T. Amelioration of scopolamine induced cognitive dysfunction and oxidative stress by *Inonotus obliquus* - a medicinal mushroom. Food Funct 2011;2:320-7.
    PUBMED | **CROSSREF**

13. Han Y, Nan S, Fan J, Chen Q, Zhang Y. *Inonotus obliquus* polysaccharides protect against Alzheimer's disease by regulating Nrf2 signaling and exerting antioxidative and antiapoptotic effects. Int J Biol Macromol 2019;131:769-78.
    PUBMED | CROSSREF

14. Jeong JH, Kim SH, Park MN, Park JY, Park HY, Song CE, Moon JH, Choi A, Kim KD, Lee NS, et al. Water extract of mixed mushroom mycelia grown on a solid barley medium is protective against experimental focal cerebral ischemia. Curr Issues Mol Biol 2021;43:365-83.
    PUBMED | CROSSREF

15. Kou RW, Han R, Gao YQ, Li D, Yin X, Gao JM. Anti-neuroinflammatory polyoxygenated lanostanoids from Chaga mushroom *Inonotus obliquus*. Phytochemistry 2021;184:112647.
    PUBMED | CROSSREF

16. Lee MG, Kwon YS, Nam KS, Kim SY, Hwang IH, Kim S, Jang H. Chaga mushroom extract induces autophagy via the AMPK-mTOR signaling pathway in breast cancer cells. J Ethnopharmacol 2021;274:114081.
    PUBMED | CROSSREF

17. Li Y, Zhou Y, Wu J, Li J, Yao H. Phelligridin D from *Inonotus obliquus* attenuates oxidative stress and accumulation of ECM in mesangial cells under high glucose via activating Nrf2. J Nat Med 2021;75:1021-9.
    PUBMED | CROSSREF

18. Szychowski KA, Skóra B, Pomianek T, Gmiński J. *Inonotus obliquus* - from folk medicine to clinical use. J Tradit Complement Med 2020;11:293-302.
    PUBMED | CROSSREF

19. Zou CX, Dong SH, Hou ZL, Yao GD, Lin B, Huang XX, Song SJ. Modified lanostane-type triterpenoids with neuroprotective effects from the fungus *Inonotus obliquus*. Bioorg Chem 2020;105:104438.
    PUBMED | CROSSREF

20. Zou CX, Wang XB, Lv TM, Hou ZL, Lin B, Huang XX, Song SJ. Flavan derivative enantiomers and drimane sesquiterpene lactones from the *Inonotus obliquus* with neuroprotective effects. Bioorg Chem 2020;96:103588.
    PUBMED | CROSSREF

21. Zhu ZY, Liu XC, Fang XN, Sun HQ, Yang XY, Zhang YM. Structural characterization and anti-tumor activity of polysaccharide produced by *Hirsutella sinensis*. Int J Biol Macromol 2016;82:959-66.
    PUBMED | CROSSREF

22. Liu M, Liu Y, Cao MJ, Liu GM, Chen Q, Sun L, Chen H. Antibacterial activity and mechanisms of depolymerized fucoidans isolated from *Laminaria japonica*. Carbohydr Polym 2017;172:294-305.
    PUBMED | CROSSREF

23. Ahmad A, Ali T, Park HY, Badshah H, Rehman SU, Kim MO. Neuroprotective effect of fisetin against amyloid-beta-induced cognitive/synaptic dysfunction, neuroinflammation, and neurodegeneration in adult mice. Mol Neurobiol 2017;54:2269-85.
    PUBMED | CROSSREF

24. Liu Y, Hettinger CL, Zhang D, Rezvani K, Wang X, Wang H. The proteasome function reporter GFPu accumulates in young brains of the APPswe/PS1dE9 Alzheimer's disease mouse model. Cell Mol Neurobiol 2014;34:315-22.
    PUBMED | CROSSREF

25. Barrachina M, Castaño E, Dalfó E, Maes T, Buesa C, Ferrer I. Reduced ubiquitin C-terminal hydrolase-1 expression levels in dementia with Lewy bodies. Neurobiol Dis 2006;22:265-73.
    PUBMED | CROSSREF

26. Choi J, Levey AI, Weintraub ST, Rees HD, Gearing M, Chin LS, Li L. Oxidative modifications and down-regulation of ubiquitin carboxyl-terminal hydrolase L1 associated with idiopathic Parkinson's and Alzheimer's diseases. J Biol Chem 2004;279:13256-64.
    PUBMED | CROSSREF

27. Lonskaya I, Hebron ML, Desforges NM, Schachter JB, Moussa CE. Nilotinib-induced autophagic changes increase endogenous parkin level and ubiquitination, leading to amyloid clearance. J Mol Med (Berl) 2014;92:373-86.
    PUBMED | CROSSREF

28. Pugazhenthi S, Qin L, Reddy PH. Common neurodegenerative pathways in obesity, diabetes, and Alzheimer's disease. Biochim Biophys Acta BBAMol Basis Dis 2017;1863:1037-45.
    PUBMED | CROSSREF

29. Lu X, Chen H, Dong P, Fu L, Zhang X. Phytochemical characteristics and hypoglycaemic activity of fraction from mushroom *Inonotus obliquus*. J Sci Food Agric 2010;90:276-80.
    PUBMED | CROSSREF

30. Ma L, Chen H, Dong P, Lu X. Anti-inflammatory and anticancer activities of extracts and compounds from the mushroom *Inonotus obliquus*. Food Chem 2013;139:503-8.
PUBMED | CROSSREF

31. Correia SC, Santos RX, Carvalho C, Cardoso S, Candeias E, Santos MS, Oliveira CR, Moreira PI. Insulin signaling, glucose metabolism and mitochondria: major players in Alzheimer's disease and diabetes interrelation. Brain Res 2012;1441:64-78.
PUBMED | CROSSREF

32. Paul S. Dysfunction of the ubiquitin-proteasome system in multiple disease conditions: therapeutic approaches. BioEssays 2008;30:1172-84.
PUBMED | CROSSREF

33. Belfiore R, Rodin A, Ferreira E, Velazquez R, Branca C, Caccamo A, Oddo S. Temporal and regional progression of Alzheimer's disease-like pathology in 3xTg-AD mice. Aging Cell 2019;18:e12873.
PUBMED | CROSSREF

34. Watanabe T, Hikichi Y, Willuweit A, Shintani Y, Horiguchi T. FBL2 regulates amyloid precursor protein (APP) metabolism by promoting ubiquitination-dependent APP degradation and inhibition of APP endocytosis. J Neurosci 2012;32:3352-65.
PUBMED | CROSSREF

35. Borgegård T, Gustavsson S, Nilsson C, Parpal S, Klintenberg R, Berg AL, Rosqvist S, Serneels L, Svensson S, Olsson F, et al. Alzheimer's disease: presenilin 2-sparing γ-secretase inhibition is a tolerable Aβ peptide-lowering strategy. J Neurosci 2012;32:17297-305.
PUBMED | CROSSREF

36. Garcia-Alloza M, Robbins EM, Zhang-Nunes SX, Purcell SM, Betensky RA, Raju S, Prada C, Greenberg SM, Bacskai BJ, Frosch MP. Characterization of amyloid deposition in the APPswe/PS1dE9 mouse model of Alzheimer disease. Neurobiol Dis 2006;24:516-24.
PUBMED | CROSSREF

37. Ringman JM, Frautschy SA, Cole GM, Masterman DL, Cummings JL. A potential role of the curry spice curcumin in Alzheimer's disease. Curr Alzheimer Res 2005;2:131-6.
PUBMED | CROSSREF

38. Nalivaeva NN, Turner AJ. Targeting amyloid clearance in Alzheimer's disease as a therapeutic strategy. Br J Pharmacol 2019;176:3447-63.
PUBMED | CROSSREF

39. Liu Y, Lashuel HA, Choi S, Xing X, Case A, Ni J, Yeh LA, Cuny GD, Stein RL, Lansbury PT Jr. Discovery of inhibitors that elucidate the role of UCH-L1 activity in the H1299 lung cancer cell line. Chem Biol 2003;10:837-46.
PUBMED | CROSSREF

40. Gentier RJ, van Leeuwen FW. Misframed ubiquitin and impaired protein quality control: an early event in Alzheimer's disease. Front Mol Neurosci 2015;8:47.
PUBMED | CROSSREF

41. Keller JN, Hanni KB, Markesbery WR. Impaired proteasome function in Alzheimer's disease. J Neurochem 2000;75:436-9.
PUBMED | CROSSREF

42. López Salon M, Morelli L, Castaño EM, Soto EF, Pasquini JM. Defective ubiquitination of cerebral proteins in Alzheimer's disease. J Neurosci Res 2000;62:302-10.
PUBMED | CROSSREF

43. Gong B, Cao Z, Zheng P, Vitolo OV, Liu S, Staniszewski A, Moolman D, Zhang H, Shelanski M, Arancio O. Ubiquitin hydrolase Uch-L1 rescues beta-amyloid-induced decreases in synaptic function and contextual memory. Cell 2006;126:775-88.
PUBMED | CROSSREF

44. Saido T, Leissring MA. Proteolytic degradation of amyloid β-protein. Cold Spring Harb Perspect Med 2012;2:a006379.
PUBMED | CROSSREF

45. Layfield R, Lowe J, Bedford L. The ubiquitin-proteasome system and neurodegenerative disorders. Essays Biochem 2005;41:157-71.
PUBMED | CROSSREF

46. Ross CA, Pickart CM. The ubiquitin-proteasome pathway in Parkinson's disease and other neurodegenerative diseases. Trends Cell Biol 2004;14:703-11.
PUBMED | CROSSREF

47. Uddin MS, Mamun AA, Jakaria M, Thangapandiyan S, Ahmad J, Rahman MA, Mathew B, Abdel-Daim MM, Aleya L. Emerging promise of sulforaphane-mediated Nrf2 signaling cascade against neurological disorders. Sci Total Environ 2020;707:135624.
PUBMED | CROSSREF

48. Upadhya SC, Hegde AN. Ubiquitin-proteasome pathway components as therapeutic targets for CNS maladies. Curr Pharm Des 2005;11:3807-28.
   PUBMED | CROSSREF

49. Lonskaya I, Shekoyan AR, Hebron ML, Desforges N, Algarzae NK, Moussa CE. Diminished parkin solubility and co-localization with intraneuronal amyloid-β are associated with autophagic defects in Alzheimer's disease. J Alzheimers Dis 2013;33:231-47.
   PUBMED | CROSSREF

50. Khandelwal PJ, Herman AM, Hoe HS, Rebeck GW, Moussa CE. Parkin mediates beclin-dependent autophagic clearance of defective mitochondria and ubiquitinated Aβ in AD models. Hum Mol Genet 2011;20:2091-102.
   PUBMED | CROSSREF

51. Hegde AN, Inokuchi K, Pei W, Casadio A, Ghirardi M, Chain DG, Martin KC, Kandel ER, Schwartz JH. Ubiquitin C-terminal hydrolase is an immediate-early gene essential for long-term facilitation in Aplysia. Cell 1997;89:115-26.
   PUBMED | CROSSREF

52. Solano RM, Casarejos MJ, Gómez A, Perucho J, de Yébenes JG, Mena MA. Parkin null cortical neuronal/glial cultures are resistant to amyloid-β1-42 toxicity: a role for autophagy? J Alzheimers Dis 2012;32:57-76.
   PUBMED | CROSSREF

53. Zhang M, Cai F, Zhang S, Zhang S, Song W. Overexpression of ubiquitin carboxyl-terminal hydrolase L1 (UCHL1) delays Alzheimer's progression *in vivo*. Sci Rep 2014;4:7298.
   PUBMED | CROSSREF